

Received October 31, 2019, accepted November 19, 2019, date of publication November 25, 2019,
date of current version December 10, 2019.

Digital Object Identifier 10.1109/ACCESS.2019.2955566

Fast Recognition and Location of Target Fruit Based on Depth Information

YUYU TIAN¹, HUICHUAN DUAN¹, RONG LUO², YAN ZHANG³, WEIKUAN JIA¹,
JIAN LIAN⁴, YUANJIE ZHENG¹, CHENGZHI RUAN⁵, AND CHENGJIANG LI⁴

¹School of Information Science and Engineering, Shandong Normal University, Jinan 250358, China

²School of Light Industry Science and Engineering, Qilu University of Technology, Jinan 250351, China

³College of Industry and Commerce, Shandong Management University, Jinan 250357, China

⁴Department of Electrical Engineering and Information Technology, Shandong University of Science and Technology, Jinan 250031, China

⁵College of Mechanical and Electrical Engineering, Wuyi University, Wuyishan 354300, China

Corresponding authors: Huichuan Duan (hcdan@sdu.edu.cn) and Weikuan Jia (jwk_1982@163.com)

This work was supported in part by the Focus on Research and Development Plan in Shandong Province under Grant 2019GNC106115, in part by the China Postdoctoral Science Foundation under Grant 2018M630797, in part by the National Nature Science Foundation of China under Grant 31571571, Grant 21978139, and Grant 61903288, in part by the Fujian Province Outstanding Young Scientists Training Project (Fujian T&R (2018) No. 47), and in part by the Taishan Scholar Program of Shandong Province of China under Grant TSHW201502038.

ABSTRACT In order to realize the recognition and localization of the target fruit more accurately and efficiently, an optimized graph-based recognition algorithm based on image depth information is proposed. Firstly, the gradient information of the depth image is obtained from the acquired depth apple image, the gradient vector is reflected from the 3D space to the 2D space, and then rotated 90 degrees clockwise, and the regular region forms the center of the vortex, which is the target fruit center to determine target fruit location. In the RGB space, the graph-based segmentation algorithm is introduced. By constructing the adaptive threshold, the mapping relationship between the number of centers and the parameters of k and \min is established to find the target fruit region. Finally, scan the maximum radius of the super pixel area where the center of the circle is located, and fit the target fruit to realize the recognition and localization of the apple. The experimental results show that the target recognition rate is 96.61%, and the recognition time has been reduced significantly.

INDEX TERMS Target fruit, depth image, graph segmentation, predicate optimization.

I. INTRODUCTION

Machine vision system as the “eyes” of agricultural robots, used to sense their complex environmental information, and achieve the target identification and location, has been widely used to estimate fruit and vegetable yield [1]–[3], target recognition of picking robot [4]–[6], crop growth monitoring [7]–[9], and so on, in order to realize scientific management of agricultural production. Achieve the accurate identification of the fruit and rapid positioning, will directly affect the real-time and reliability of picking robot, therefore, how to realize the goal the accurate identification and positioning of the fruit to be key to the study of the visual system, attracted the attention of many scholars. Under natural conditions, actual apple orchard environment is relatively complex,

which bring the bigger challenges for apple picking robot. In recent years, whether using monocular vision system [10], or a binocular vision system [11], [12]; Whether a single fruit [13], [14] or overlapping shade fruit [15], [16]; Both static fruit [17] and dynamic target [18] recognition has made great progress, but for now, cannot meet the needs of the fast picking robot visual servo control. Accurate identification and rapid positioning of apple picking robot vision system, is still the research emphasis and difficulty. In order to further improve the operation effect of picking robot, meet the real-time need of picking work, to better alleviate the contradiction between recognition accuracy and efficiency, need to be further optimized recognition algorithm.

In order to better alleviate the contradiction between recognition accuracy and positioning efficiency, an optimizational graph-based recognition algorithm based on image depth information is proposed in this paper. Firstly, the depth image

The associate editor coordinating the review of this manuscript and approving it for publication was Shuihua Wang¹.

and RGB image of apple fruit were collected by Kinect camera. Using the gradient field information of the apple depth image, the gradient vector is rotated 90 degrees clockwise by two-dimensional projection, and the obtained vortex center is the target fruit center to determine the target fruit position. Then, in the RGB image, the graph segmentation algorithm is introduced. By constructing the predicate evaluation adaptive threshold of the constraint mechanism, the mapping relationship between the number of centers and k and \min parameters is established, and the automatic segmentation of the apple image is realized to obtain the target fruit region. Finally, according to the maximum radius scan of the super pixel area where the center of the circle is scanned, the contour of the target fruit is fitted to achieve efficient identification and localization of the target fruit. The new method breaks the tradition of identifying and relocating before. The new method does not need to extract the target fruit features, and does not need to design a classifier. First, find the center of the circle and then fit the contour to improve the recognition efficiency.

In general, this study offers at least the following contribution as:

- (I) To the best of our knowledge, this is an early work for introducing depth information to locate the center of the target fruit.
- (II) A novel automated segmentation algorithm is established based on the guidance of the number of fruit centers.
- (III) The proposed method outperforms the state-of-the-art techniques in accuracy and efficiency of target fruits recognition.

The rest of this paper is organized as follows, we first provide the related works and data acquisition in section II. In the section III, we present the details of the method of locating the center of fruit, the new method is based on the depth images. In section IV, based on the optimized graph segmentation algorithm, an automatic segmentation method is proposed, which is guided by the number of circles. Combined with the center location and region segmentation, the target fruit can be located quickly and accurately. In section V, the experiment is arranged, the performance of new method is evaluated from multiple perspectives, such as recognition rate, recognition times, recognition rate of fruit with different postures. In section VI, the conclusion and future works are provide.

II. RELATED WORKS AND DATA ACQUISITION

A. RELATED WORKS

At present, the information technology rapid development, for the target recognition of apple fruit is both a challenge and opportunity, many scholars have made gratifying achievements. Kelman and Linker through convexity of fruit tree image detection, determine the apple edges, and use the method of least square constraint mechanism for 3 d modeling, for a single and overlapping apple to locate respectively, accuracy of up to 94% [19]. Wachs *et al.* using the

infrared image and color image two forms of maximum mutual information to extract the high- and low-level visual features, and detect “green” apples in the fruit tree canopy background image, two kinds feature recognition rate can be up to 54% and 74% respectively [20]. Liu *et al.* proposed a recognition method of apples in plastic bags based on bock classification, watershed algorithm is adopted to segment original images into irregular block, and then these blocks are classified into fruit blocks and non-fruit blocks by VSM, the new method can restrain the interference of light [21]. Xu and Lv used R-G color differences to process apple images, the images is segmented by PCNN based on minimum cross entropy, an improved random Hough transform method is used to detect the characteristic circle, according to the edge of the apple target obtained by the SUSAN edge detection algorithm, 93% of apples were accurately identified [22]. Moallem *et al.* combines a variety of machine learning methods to classify apple fruits [23]. Ji *et al.* focuses on establishing apple viscoelastic finite element complex model to estimate apple stress variation during grasping with its own characteristics of constant velocity and continuous energy input [24], [25].

The above research results are mostly adopting the conventional image processing method, firstly, the image is segmented, the target fruit features are extracted, and finally the classifier is designed to identify the target fruit. Although these methods solve the recognition accuracy of apple’s target fruit to a certain extent, some algorithms have higher complexity and poor recognition efficiency, which cannot meet the needs of real-time operation of picking robots.

It is the efforts of these scholars that push the research of harvesting robot forward. Furthermore, more target fruit recognition techniques will provide theoretical reference for this study [26]–[31].

B. IMAGE ACQUISITION

The image of Apple’s image was collected at the Longwangshan Apple Production Base in Fushan District, Yantai City, Shandong Province (Agricultural Information Technology Experimental Base of Shandong Normal University). All images were collected under natural light conditions (including front lighting and backlighting). The apple variety was Red Fuji.

Image acquisition lens: Kinect V2(Microsoft), the RGB image acquisition resolution is 1920*1080, the depth image resolution is 512*424, and the output format is JPG.

Image acquisition method: Each sample sampling point outputs the RGB and depth images of the target fruit at the same time, as shown in Figure 1. (To facilitate the identification of the target fruit, when the depth image and RGB image are collected in this study, the resolution is uniformly set to 512.*424). When acquiring a depth image, the Kinect camera collects every point in the field of view and forms a depth of field image representing the surrounding environment.

According to the working principle of Kinect, the depth sensor senses the surrounding environment by means of black

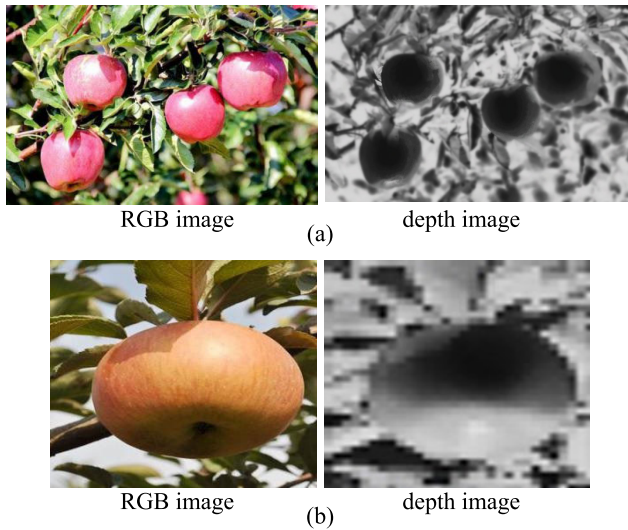


FIGURE 1. Two image patterns acquired at the same sample point.

and white spectrum. In the obtained depth image, the deeper the black is, the closer the target is; the lighter the white is, the farther the target is. The gray area between the black and white represents the physical distance between the target and the sensor.

Due to the changeable natural growth posture of apple fruits and the shooting angle caused by the picking robot's position, the apple images collected by the picking robot's visual system are diverse, such as single unshaded fruit, branches and leaves covered fruit, overlapping fruit, etc. A total of 150 apple images were collected in this study, including 236 target fruits, including 61 overlapped fruits, 47 fruits covered by branches and leaves, and 128 single uncovered fruits.

C. METHOD OVERVIEW

In the research of fruit and vegetable picking robot, the precise identification and efficient location of target fruit is still a difficult problem. In the past, apple target fruit positioning mostly adopts target recognition first, and then finds the center of target fruit on the basis of recognition, so as to achieve accurate positioning of target fruit. Such methods are difficult to meet the real-time operation requirements of picking robots in terms of time and efficiency.

In order to realize efficient and accurate identification and positioning of target fruits and meet the needs of visual servo of picking robot, this study tries to conduct target fruit positioning first and then target fruit contour fitting. The new method first uses the acquired depth image of the target fruit, and obtains the isobath map and gradient projection of the target image by using the gradient field information of the depth image, the vorticity center of the target region is obtained by gradient rotation, so the center location of the target fruit is realized. Then, use the collected RGB images and have the aid of graph segmentation algorithm, an automatic segmentation algorithm of apple images is constructed by designing a

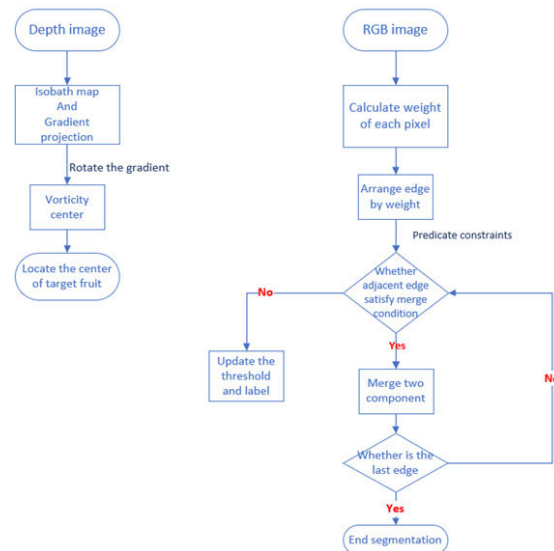


FIGURE 2. Flow chart of new target rapid identification and positioning method.

new predicate evaluation and constraint mechanism, so as to obtain the target fruit area. By scanning the maximum radius of the superpixel region from the center of the target fruit circle and the approximate area, the outline of the target fruit is finally obtained, so as to realize the rapid identification and positioning of the apple target fruit. The specific process is shown in figure 2.

III. TARGET FRUIT POSITIONING BASED ON DEPTH INFORMATION

In the complex background image, in order to further eliminate the influence of background and illumination, this study tries to find the center of the target fruit by using the depth information of the image. Using the depth information of the image of the target fruit, the isobath image of the depth image is drawn, the gradient field of the target image is analyzed by the iso-depth information, and then the three-dimensional gradient information of the depth image is projected in a two-dimensional plane, and the two-dimensional gradient projection direction of the target fruit region is more uniform and orderly, while the gradient direction of the background region is more disorderly. Then, the two-dimensional gradient direction is rotated clockwise by 90 degrees, and a uniform and orderly gradient region can obtain a vorticity center, and each concentrated vorticity center is the center of the target fruit, and the center of the target fruit is positioned.

A. ISOBATH MAP ACQUISITION

According to the depth sensor principle, in the obtained depth image, the pixel point closer to the camera has a smaller distance value, for the target fruit, the pixel distance of the center point of the target fruit is small, and the peripheral distance value of the target fruit is relatively large. Using the depth information mapped by the depth image, the three-dimensional geometric feature of the target image is

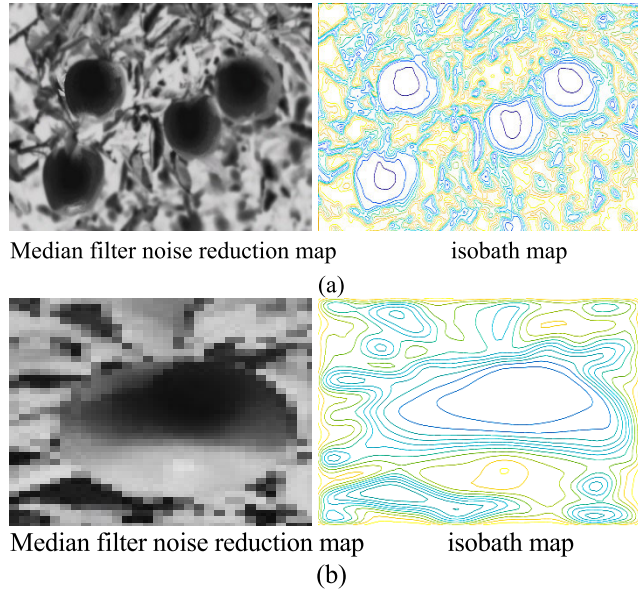


FIGURE 3. Preprocessed apple depth images and iso-level contour map of apples fruit using mapped depth values.

calculated, and draw the isobath curve of the depth image, that is, the isobath map of the target image, based on the distance from the pixel to the camera.

The original depth image acquired is relatively fuzzy, which is easy to interfere with the drawing of the isobath curve. To obtain the isobath map of the target image better, the median filtering algorithm is used to smooth the original depth image. Taking 1(b) as an example, 3×3 median filtering is used to denoise, and the obtained image is shown in Fig. 3(a). After noise reduction, the target edge is smooth and the burr is significantly reduced. The isobath curve of the noise reduction map 3(a) is drawn with a distance difference of 0.5 cm to obtain an isobath image of the target image, as shown in Fig. 3(b).

B. GRADIENT INFORMATION OF DEPTH IMAGE

It can be seen from the characteristics of the depth image that the pixel point closer to the camera has a smaller distance value, and for the target fruit area of the depth image, the distance value of the center of the fruit is smaller, and the target peripheral distance value is relatively larger. Quantify the depth information of the target image, as shown in Equation 1.

$$\vec{V} = \nabla D = \left(\frac{\partial D}{\partial x}, \frac{\partial D}{\partial y} \right) = (u, v) \quad (1)$$

where \vec{V} represents a set of vectors (u, v) on the gradient vector field in three-dimensional space. u, v respectively represent the partial derivative of the depth D in the x, y direction in the three-dimensional coordinates, that is, the gradient direction of the target fruit. Find the gradient in all directions from the smallest pixel.

Since the surface of the target fruit is convex parabola, the three-dimensional gradient information of the depth image is

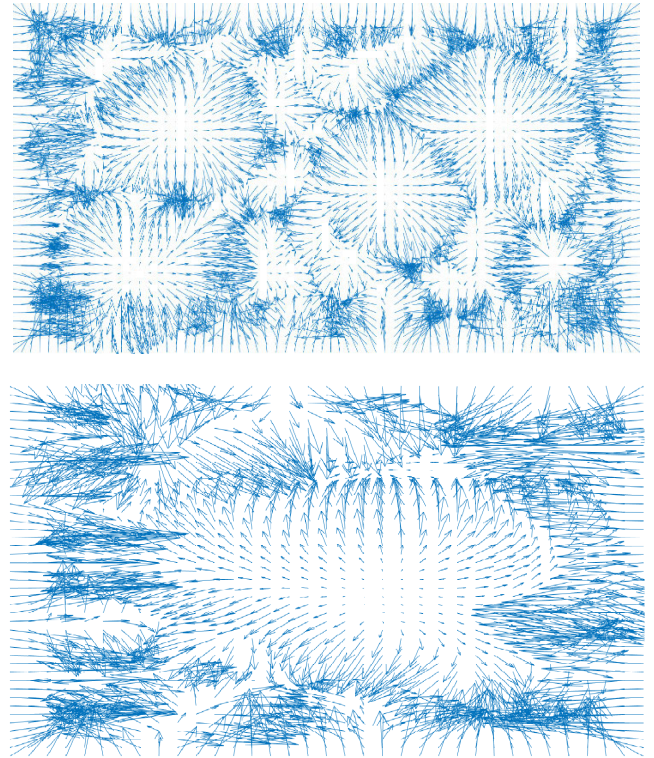


FIGURE 4. Gradient field direction projection.

projected onto the two-dimensional iso-depth plane, and the obtained direction vector appears outwardly divergent along the surface of the target fruit in the gradient field, as shown in figure 4.

As can be seen from figure 4, in the two-dimensional gradient projection view, the gradient direction arrangement of the target fruit region is relatively regular and orderly, showing a state of diverging from the inside to the outside. In the non-target area, because the background is relatively complex, the background area depth information is slightly cluttered, so the gradient vector of the background is relatively disorderly. That is, in the gradient vector projection map, the target fruit region is regularly ordered, and the background region vector is disorderly and disorderly.

C. VORTICITY CENTER POSITION

Vorticity was originally a concept in meteorology and was introduced into the center of the circle by this study. The vorticity is a three-dimensional vector, the rotation of the velocity field, considering only the vertical component of the vorticity, the vorticity component that rotates around the vertical axis. In this study, the vertical component is the gradient vector and the vertical axis is the isobath. By uniformly rotating all the gradient vectors in Fig. 4 by 90° in a clockwise direction at a fixed origin, the angular velocity of the pixel (direction only) referenced by the adjacent vector is

$$\omega' = \nabla \times \vec{V} = \left(\frac{\partial}{\partial x}, \frac{\partial}{\partial y}, \frac{\partial}{\partial z} \right) \times (u, v, 0) = \left(\frac{\partial u}{\partial x} - \frac{\partial v}{\partial y} \right) \vec{z} \quad (2)$$

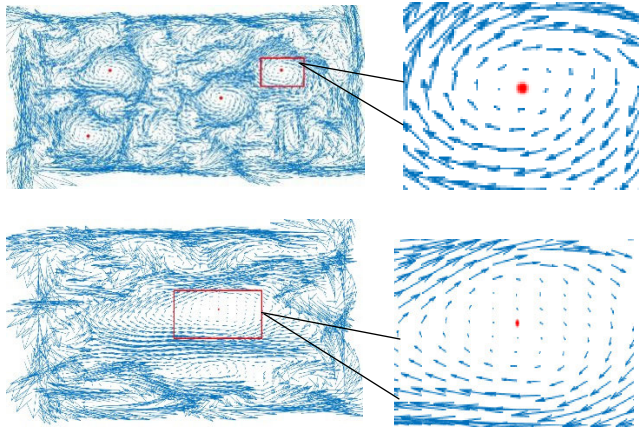


FIGURE 5. Target image vorticity center map (red points is the center of circle).

where ∇ is a partial derivative operator in the x, y, z direction, and \vec{z} is a vector in the z -axis direction. Because the speed of the vortex changes

$$\omega = \frac{\phi}{t} \quad (3)$$

where ϕ represents the arc length (similar to the vector size) and t represents the same time.

In the two-dimensional projection, the gradient vector that originally is convexly parabolic surface is rotated clockwise, and the center of the target fruit region forms a vortex. The gradient vector that originally is concave parabolic surface rotates counterclockwise, furthermore, the background region is chaotic. In the target depth image, the maximum vorticity is obtained at the fastest distance change, so the maximum angular velocity is location of the center of the circle, as shown in figure 5.

It can be seen from figure 1 and 5 that the region where the rule is regular and the vortex is the largest is the target fruit region, vortex which in disorder is the background area, and the center of the vorticity is the center of the target fruit. At this point, the center of the realistic target fruit is positioned, and on this basis, the contour of the target fruit is further fitted.

IV. TARGET REGION FITTING BASED ON OPTIMIZED GRAPH

In Section 3, the depth information of the image has been used to located the center of the target fruit. In the apple image, the target fruit can be regarded as a circle, based on the known circle's center, the target fruit's radius is further searched, and the target fruit region is fitted. Therefore, the next research focus shifts to recognize the target area, that is, to achieve efficient and accurate segmentation for the target image, and to find an proper segmentation algorithm to divide the apple image into several regions, moreover the region where the circle's center located is the region of the target fruit. Furthermore, search for the correspondence between the target region and the target radius to achieve to fit contour of the target fruit.

In the RGB space, because the background of apple images are complex, and the conventional segmentation algorithm with stationary threshold is not ideal, such as segmentation algorithm based on threshold or improved threshold [32], [33], K-means clustering [34]–[36], Otsu method [37], [38], etc.. This study attempts to construct an adaptive threshold segmentation method based on the graph segmentation algorithm [39]–[43], achieve efficient and adaptive segmentation through predicate constraints.

A. PRINCIPLE OF THE GRAPH SEGMENTATION

The most straightforward way to find the approximate region of the target fruit region is the reliable segmentation algorithm. In general, the focus of segmentation is more on the target fruit itself than on the segmentation algorithm's parameter optimization. The image consists of corresponding pixels. The graph consists of vertex sets called V (vertices) and edge sets called E (edges), denoted as $G = (V, E)$, and each vertex $v \in V$ is a single pixel; the edges connecting a pair of vertices (v_i, v_j) has its weight $w(v_i, v_j)$, which means a measure of dissimilarity between two vertices, which consist an undirected graph. There is a path between the two vertices. A graph without a loop is called the Tree. The tree with the smallest sum of edge weights is called the minimum spanning tree (MST). The segmentation of this study is in the RGB space, where the similarity between two points is defined using the RGB distance.

$$S = \sqrt{(r_1 - r_2)^2 + (g_1 - g_2)^2 + (b_1 - b_2)^2} \quad (4)$$

Based on the concept of graph theory, let the input picture be $G(V, E)$, with M vertex called v and N side called e , according to the dissimilarity, sort the weights like e_1, e_2, \dots, e_N . We defined a segmentation evaluation mechanism to control whether the pixels are merged: starting from edge e_1 , if the two vertices from the edge are not in the same region and satisfy the merge condition, and the two pixels will be merged; if not, the threshold and region label will be updated until the condition is met, when all the edges are searched, end the merging. The detailed algorithm steps based on graph segmentation are:

Step 1 Calculate the degree of dissimilarity between each pixel and its 4 fields or 8 fields;

Step 2 Arrange according to the degree of dissimilarity from small to large, as e_1, e_2, \dots, e_N ;

Step 3 Select e_i to compare the currently selected edge e_j to determine whether to merge.

Step 4 Update the threshold and class label;

Step 5 If $i < n$, in the updated order, select the next edge, turn to Step 3, otherwise end.

B. SELECT COLOR CHANNEL

When using the graph segmentation algorithm for apple image segmentation, susceptible to light intensity, when robot work at orchard, light environment is uncontrollable factors. Different color space for lighting, material conversion

conditions with different sensitivities, as standard RGB are sensitive to shadows and highlights; opponent color space not sensitive to bright edge, but sensitive to the geometric edge and shadow, normalized RGB space is insensitive to the shadow and the shadow edges, but still highly sensitive to highlights. The hue H is the most constant and is insensitive to shadows, shadow edges, and highlights, most robust to the influence of light intensity change.

C. AUTOMATED SEGMENTATION ASSESSMENT CONSTRAINTS

Defines the predicate D to assess whether there is a boundary between two components in the segmentation. This predicate is based on measuring the difference between elements along the boundaries of two components, relative to measuring the difference between adjacent elements within two components. The resulting predicate compares the differences between components and the differences within the component to adaptive adjust with the local characteristics of the data.

We define an intra-component difference assessment criterion, let $C \subseteq V$, for a region (an area in graph theory is a minimum spanning tree) is the maximum weight in the region, as shown in Equation 5. That is, the given component C will consider to connect at least when the weight is $\text{Int}(C)$. And we define an difference assessment criteria of different adjacent component, let $C_1, C_2 \subseteq V$ to connect the minimum weight edges of the two component, that is, the dissimilarity of the edges with the least dissimilarity among all the edges which connected the two component, as shown in Equation 6. If there is no edge connected, then $\text{Dif}(C_1, C_2)$ is ∞ .

$$\text{Int}(C) = \max_{e \in \text{MST}(C, E)} w(e) \quad (5)$$

$$\text{Dif}(C_1, C_2) = \max_{e \in \text{MST}(C, E)} w((v_i, v_j)) \quad (6)$$

Component comparison predicate evaluate whether there is a boundary between a pair or components by checking whether the difference between the components is greater than the difference between the at least one component and the interior. The threshold function is used to control the extent to which the difference between components must be larger than the minimum internal difference.

$$D(C_1, C_2) = \begin{cases} \text{ture,} & \text{if } \text{Dif}(C_1, C_2) > M \text{Int}(C_1, C_2) \\ \text{false,} & \text{otherwise} \end{cases} \quad (7)$$

where the minimum internal difference $M\text{Int}$ is defined as

$$M \text{Int}(C_1, C_2) = \min(\text{Int}(C_1) + \tau(C_1), \text{Int}(C_2) + \tau(C_2)) \quad (8)$$

The threshold function controls the degree that the difference between the two components must be greater than their internal differences, so there is evidence that there is a boundary between them (D is true). But for small components, $\text{Int}(C)$ does not estimate the local characteristics of the data well. In extreme cases, when $|C| = 1$, $\text{Int}(C) = 0$. Therefore,

we use a threshold function based on the size of component, as shown in the following Equation,

$$\tau(C) = \frac{k}{|C|} \quad (9)$$

where $|C|$ represents the pixel value of component C , and k is a constant parameter, indicates how many components the image will be divided into. In practice, we have found that a larger k leads to a preference for larger components, and the change in k is logarithmic positive with the number of apples in the segmented image. In order to achieve automatic segmentation of the target apple image, the parameter of k is calculated as follows,

$$k = 30 \log_2 N + 90 \quad (10)$$

where N is the number of apples in the segmented image, ie the number of centroid points obtained in the previous chapter. But please note that k is not the smallest component size. Smaller components are allowed when there is a large enough difference between adjacent components. By observing and calculating the 10 minimum target area of the data set, obtained by Matlab statistical average value of about 500. Then the minimum area $\min = 500$ in the segmentation process is specified.

D. TARGET AREA IDENTIFICATION

Combining the depth image and the RGB image of the same sample point, the target fruit center is accurately positioned in the depth image mode, and the target fruit segmentation is completed in the RGB image mode, and the segmentation region where the center of the circle is located is the target fruit region, thereby achieving the fruit identification and localization. In order to achieve the target fruit recognition more efficiently and accurately, the target radius is searched in the super pixel area where the center of the circle is located, and the edge of the segment is scanned from the center of the circle to obtain the maximum radius of the target area. The target fruit contour is fitted by the center position and the maximum radius, as shown in figure 7, and finally the target fruit is accurately identified and positioned.

It is notable that, the proposed method relates to the following areas including graphics [41], [42], [44]–[47], multimedia [40], [48]–[54], automation control [55]–[58], classification [59]–[62], image fusion [63], [64], image retrieval [65]–[70], and other fruit recognition [71]–[75].

V. EXPERIMENTAL ANALYSIS

A. EXPERIMENTAL DESIGN

The collected 150 images were used as experimental data to verify the algorithm which the target fruits included a single unobstructed fruit, overlapping fruits, and foliage blocking fruit. The performance of the identification method is measured from the indicators such as correct recognition rate, misrecognition rate, missed rate, and recognition time. The recognition rate refers to the ratio of the number of correctly identified fruits to the total number to be identified; the

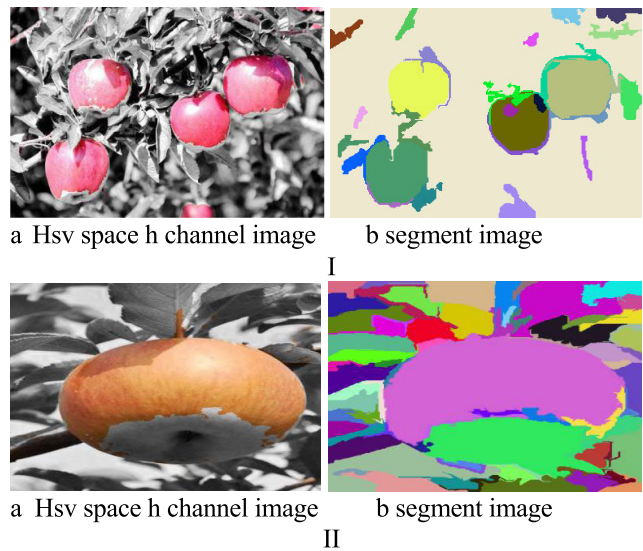


FIGURE 6. Segmented image of target fruits, where $\sigma = 0.8$, $k = 30\log_2 N + 90$, and $\min = 500$. (An optimized graph-based image segmentation algorithm was used to segment the image into k super-pixel regions, each of which was defined with different RGB colors.).



FIGURE 7. Target fruit fitting effect chart.

recognition time refers to the time taken to identify the sample to be tested with the trained model. Among them, the recognition rate is divided according to the growth posture of the fruit and the angle of image collection into three categories: unobstructed fruit, foliage blocking fruit, and overlapping fruits.

In order to verify the effectiveness of the proposed method for fruit recognition and localization better, the experiment was compared with the literature [15]–[17], [76] method.

The experimental operating environment of this research: operating system environment Win 10, computing environment MATLAB 2016a, hardware configuration is Intel (R) Core (TM) i7-6700 CUP @ 3.40GHz.

B. IDENTIFICATION METHOD VERIFICATION

From the effect of recognition, the three types of target fruits have been distinguished from the background to achieve the final recognition and positioning. It can be seen from figure 8 that the fitting effect is not ideal in an environment where large-area foliage is blocked. The occluded long-distance target fruit is easy to miss.

TABLE 1. Correct recognition rate of three types of target fruits in different methods (%).

recognition methods	Unobstructed fruit	Blocking fruit	Overlapping fruit
Method of this paper	98.43	93.62	95.08
Literature 15	96.10	87.23	86.89
Literature 16	97.61	91.49	85.25
Literature 17	95.32	89.36	86.89
Literature 79	97.66	88.61	91.75
Literature 80	96.32	87.69	90.64

C. EXPERIMENTAL RESULTS AND ANALYSIS

In order to describe more clearly the effect of recognition and localization method established in this paper, the target fruit recognition and positioning effects of three different growth postures are separately counted here, and the results are listed in Table 1.

It can be seen from Table 1 that several algorithm models can achieve good results for the recognition of unobstructed fruits. However, for the recognition of the target fruit occluded by the foliage and the other fruit, the performance of several methods is different. The new method proposed in this paper has the best recognition and localization effect, and the recognition rate of the two target fruits is 93% and 95%.

In order to further evaluate the efficiency of operating and the accuracy of positioning of the new method, the running time and recognition accuracy of each method were separately calculated. The results are shown in Table 2.

It can be seen from Table 2 that the new method has obvious advantages in aspect of recognition time and total recognition rate, and the operation effect is relatively ideal, which alleviates the contradiction between running time and recognition efficiency to some extent.

D. DISCUSSIONS

Form figure 8, table 1 & 2, and the large number of repetitive experiments, the experimental results show that, the new method has obvious recognition accuracy and efficiency. The new method can locate the center of the target fruit quickly by using depth image, as the first step of recognition, its most significant advantage is fast and accurate. The second step is apple image segmentation, which is the most time-consuming part of this method. On the basis of graph segmentation, an optimized segmentation algorithm is proposed, that is, apple images segmentation is guided by the number

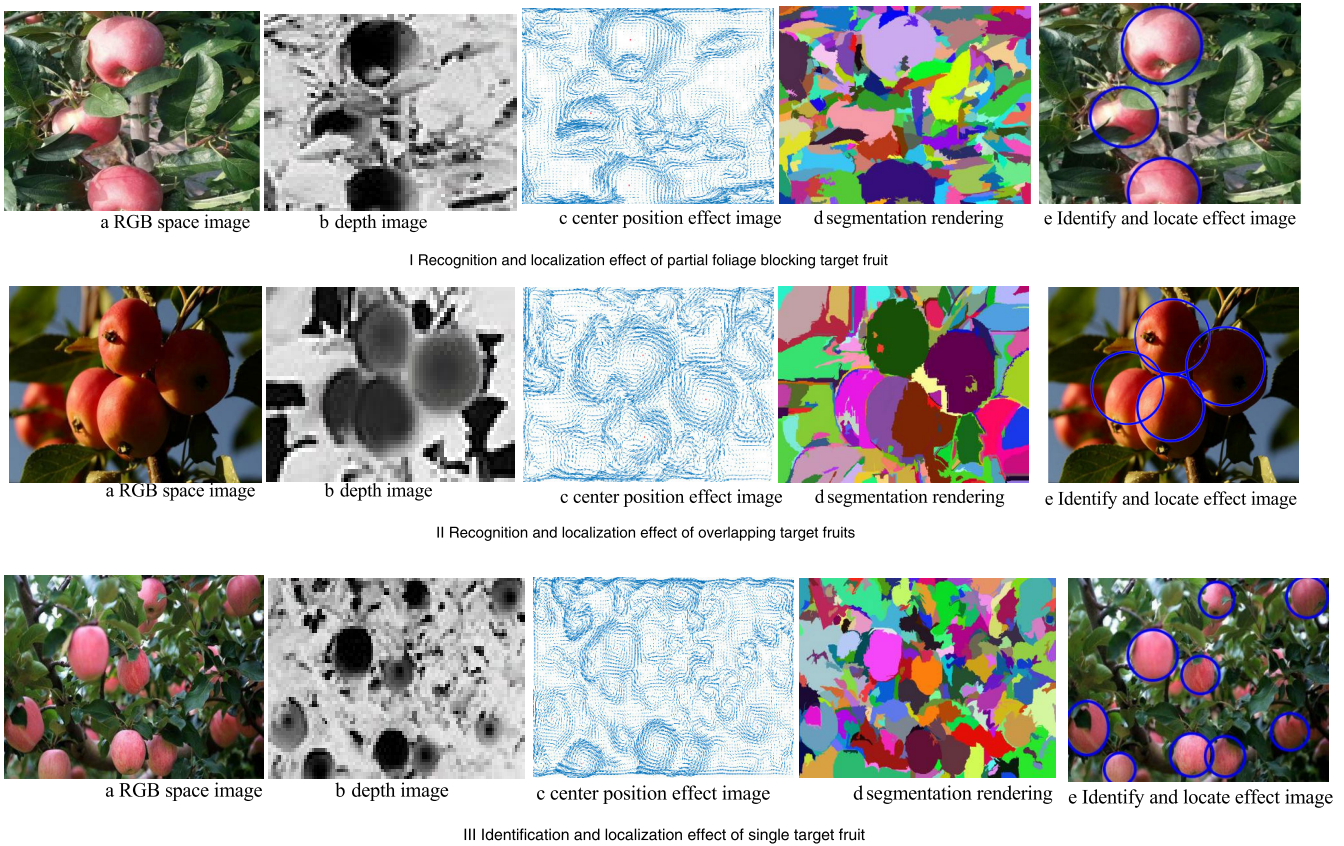


FIGURE 8. New method three types of target fruit recognition effect map.

TABLE 2. Comparison of different methods of identification and positioning performance.

recognition methods	Recognition time (s)	Total recognition rate (%)
Method of this paper	2.21	96.61
Literature 15	5.69	91.52
Literature 16	3.77	93.22
Literature 17	4.01	91.95
Literature 79	4.27	93.83
Literature 80	3.80	92.97

of centers. The results of the new segmentation method are satisfactory. Finally, combining the center and segmentation region, the target fruit fitting is achieved. The fitting effect is ideal.

The traditional recognition and location methods mostly adopt the following ways: image segmentation, feature extraction, and classifier design. That is, the target fruit is

recognized and located on the basis of the segmentation image. Generally speaking, the traditional methods cannot achieve ideal results in accuracy and efficiency. The new method in this paper adopts the thought of locating first and recognizing later, and the effect is ideal. In the future research, we will further try to optimize the segmentation or other segmentation algorithms, in order to achieve the real-time working ability of the harvesting robot.

VI. CONCLUSION

In order to improve the picking efficiency of apple picking robots, this paper studies the recognition and localization of target fruits. Firstly, the depth image and the RGB image of the same sample point are collected. In the depth image environment, the isobath map of the target image is obtained, and the gradient field information is further acquired, and the 3-dimensional gradient information is projected onto the two-dimensional plane, by rotating the gradient vector, a uniformly ordered region forms a vorticity, which is the central projection of the target fruit, achieving rapid positioning of the target fruit. In the RGB image environment, the target image segmentation is performed by method of graph optimization, which constructed the logical predicate constraint evaluation mechanism, and choose a suitable color channel. The region where the center of the circle is located is the target area. By scanning the maximum radius of the area,

the target fruit area is finally fitted to realize the recognition and localization of the target fruit.

The experimental results show that the new method is ideal in terms of operational efficiency and recognition accuracy, and it also achieves good results for leaf occlusion and overlapping target fruit recognition and localization. The new method does not need to train the model in advance, and no manual labeling is needed in the segmentation process to achieve adaptive recognition and localization of the target fruit. And largely alleviates the contradiction between recognition effect and operational efficiency.

In the future works, we will further optimize the method to find the center of target fruits, in order to obtain center more quickly. At the same time, we try to combine more suitable segmentation algorithm, in order to improve the recognition efficiency and accuracy significantly.

REFERENCES

- [1] A. Gongal, A. Silwal, M. Karkee, Q. Zhang, K. Lewis, and S. Amatya, "Apple crop-load estimation with over-the-row machine vision system," *Comput. Electron. Agricult.*, vol. 120, pp. 26–35, Jan. 2016.
- [2] M. Stein, S. Bargoti, and J. Underwood, "Image based mango fruit detection, Localisation and yield estimation using multiple view geometry," *Sensors*, vol. 16, no. 11, p. 1915, 2016.
- [3] R. Barth, J. Hemming, and E. J. van Henten, "Design of an eye-in-hand sensing and servo control framework for harvesting robotics in dense vegetation," *Biosyst. Eng.*, vol. 146, pp. 71–84, Jun. 2016.
- [4] C. W. Bac, E. J. van Henten, J. Hemming, and Y. Edan, "Harvesting robots for high-value crops: State-of-the-art review and challenges ahead," *J. Field Robot.*, vol. 31, no. 6, pp. 888–911, 2014.
- [5] Y. Zhao, L. Gong, Y. Huang, and C. Liu, "A review of key techniques of vision-based control for harvesting robot," *Comput. Electron. Agricult.*, vol. 127, pp. 311–323, Sep. 2016.
- [6] C. W. Bac, J. Hemming, B. A. J. van Tuijl, R. Barth, E. Wais, and E. J. van Henten, "Performance evaluation of a harvesting robot for sweet pepper," *J. Field Robot.*, vol. 34, no. 6, pp. 1123–1139, Sep. 2017.
- [7] R. Schima, H. Mollenhauer, I. Merbach, A. Lausch, P. Dietrich, J. Bumberger, and G. Grenzdoerffer, "Imagine all the plants: Evaluation of a light-field camera for on-site crop growth monitoring," *Remote Sens.*, vol. 8, no. 10, p. 823, 2016.
- [8] S. S. Chouhan, U. P. Singh, and S. Jain, "Applications of computer vision in plant pathology: A survey," *Arch. Comput. Methods Eng.*, to be published, doi: 10.1007/s11831-019-09324-0.
- [9] P. Tanmayee, "Rice crop monitoring system—A lot based machine vision approach," in *Proc. IEEE Int. Conf. Nextgen Electron. Technol., Silicon Softw. (ICNETS2)*, Mar. 2017, pp. 26–29.
- [10] J. Zhang, B. Yang, L. Huang, and N. Geng, "An obstacle detection system based on monocular vision for apple orchard robot," *Int. J. Robot. Autom.*, vol. 32, no. 6, pp. 639–648, 2017.
- [11] Y. Si, G. Liu, and J. Feng, "Location of apples in trees using stereoscopic vision," *Comput. Electron. Agricult.*, vol. 112, pp. 68–74, Mar. 2015.
- [12] Y. Tao and J. Zhou, "Automatic apple recognition based on the fusion of color and 3D feature for robotic fruit picking," *Comput. Electron. Agricult.*, vol. 142, pp. 388–396, Nov. 2017.
- [13] W. Ji, Z. Qian, B. Xu, and D. Zhao, "A nighttime image enhancement method based on Retinex and guided filter for object recognition of apple harvesting robot," *Int. J. Adv. Robot. Syst.*, vol. 15, no. 1, 2018, Art. no. 1729881417753871.
- [14] J. Feng, L. Zeng, and L. He, "Apple fruit recognition algorithm based on multi-spectral dynamic image analysis," *Sensors*, vol. 19, no. 4, p. 949, Feb. 2019.
- [15] J. Lv, Y. Wang, Q. Wang, H. Rong, Z. Ma, B. Yang, L. Xu, and H. Ni, "Method for discriminating of the shape of overlapped apple fruit images," *Biosyst. Eng.*, vol. 186, pp. 118–129, Oct. 2019.
- [16] W. Jia, D. Zhao, C. Ruan, and C. Hu, "Fast recognition of overlapping fruit based on maximum optimisation for apple harvesting robot," *Int. J. Collaborative Intell.*, vol. 1, no. 2, pp. 124–136, 2015.
- [17] D. Zhao, T. Shen, W. Jia, and Y. Chen, "Fast tracking and recognition of overlapping fruit for apple harvesting robot," (in Chinese), *Trans. Chin. Soc. Agricult. Eng.*, vol. 31, no. 2, pp. 22–28, 2015.
- [18] J. Lü, D. A. Zhao, and W. Ji, "Research on matching recognition method of oscillating fruit for apple harvesting robot," (in Chinese), *Trans. Chin. Soc. Agricult. Eng.*, vol. 29, no. 20, pp. 32–39, 2013.
- [19] E. Kelman and R. Linker, "Vision-based localisation of mature apples in tree images using convexity," *Biosyst. Eng.*, vol. 118, pp. 174–185, Feb. 2014.
- [20] J. P. Wachs, H. I. Stern, T. Burks, and V. Alchanatis, "Low and high-level visual feature-based apple detection from multi-modal images," *Precis. Agricult.*, vol. 11, no. 6, pp. 717–735, Dec. 2010.
- [21] X. Liu, W. Jia, C. Ruan, D. Zhao, Y. Gu, and W. Chen, "The recognition of apple fruits in plastic bags based on block classification," *Precis. Agricult.*, vol. 19, no. 4, pp. 735–749, Aug. 2018.
- [22] L. Xu and J. Lv, "Recognition method for apple fruit based on SUSAN and PCNN," *Multimedia Tools Appl.*, vol. 77, no. 6, pp. 7205–7219, 2018.
- [23] P. Moallem, A. Serajoddin, and H. Pourghassem, "Computer vision-based apple grading for golden delicious apples based on surface features," *Inf. Process. Agricult.*, vol. 4, no. 1, pp. 33–40, Mar. 2017.
- [24] W. Ji, Z. Qian, G. Chen, D. Zhao, and B. Xu, "Apple viscoelastic complex model for bruise damage analysis in constant velocity grasping by gripper," *Comput. Electron. Agricult.*, vol. 162, pp. 907–920, Jul. 2019.
- [25] W. Ji, X. Meng, B. Xu, D. Zhao, and Z. Qian, "Branch localization method based on the skeleton feature extraction and stereo matching for apple harvesting robot," *Int. J. Adv. Robot. Syst.*, vol. 14, no. 3, 2017, Art. no. 1729881417705276.
- [26] V. Bloch, A. Degani, and A. Bechar, "A methodology of orchard architecture design for an optimal harvesting robot," *Biosyst. Eng.*, vol. 166, pp. 126–137, Feb. 2018.
- [27] B. Zhang, J. Zhou, N. Zhang, B. Gu, Z. Yan, S. I. Idris, and Y. Meng, "Comparative study of mechanical damage caused by a two-finger tomato gripper with different robotic grasping patterns for harvesting robots," *Biosyst. Eng.*, vol. 171, pp. 245–257, Jul. 2018.
- [28] Y. Xiong, Y. Ge, P. J. From, and L. Grimstad, "An autonomous strawberry-harvesting robot: Design, development, integration, and field evaluation," *J. Field Robot.*, to be published.
- [29] X. Liu, D. Zhao, W. Ji, Y. Sun, and W. Jia, "A detection method for apple fruits based on color and shape features," *IEEE Access*, vol. 7, pp. 67923–67933, 2019.
- [30] W. Jia, G. Liang, J. Sun, C. Wan, and H. Tian, "Electronic nose-based technique for rapid detection and recognition of moldy apples," *Sensors*, vol. 19, no. 7, p. 1526, 2019.
- [31] W. Ji, G. Chen, B. Xu, X. Meng, and D. Zhao, "Recognition method of green pepper in greenhouse based on least-squares support vector machine optimized by the improved particle swarm optimization," *IEEE Access*, vol. 7, pp. 119742–119754, 2019.
- [32] Q. Yang, W.-N. Chen, T. Gu, H. Zhang, J. D. Deng, Y. Li, and J. Zhang, "Segment-based predominant learning swarm optimizer for large-scale optimization," *IEEE Trans. Cybern.*, vol. 47, no. 9, pp. 2896–2910, Sep. 2017.
- [33] C. Guo, R. Yang, and L. Zhao, "The internal parameter calibration based on sub-pixel threshold segment algorithm," *J. Comput. Methods Sci. Eng.*, vol. 18, no. 1, pp. 3–11, 2018.
- [34] R. Liu, H. Wang, and X. Yu, "Shared-nearest-neighbor-based clustering by fast search and find of density peaks," *Inf. Sci.*, vol. 450, pp. 200–226, Jun. 2018.
- [35] H. Zhang and L. Cao, "A spectral clustering based ensemble pruning approach," *Neurocomputing*, vol. 139, pp. 289–297, Sep. 2014.
- [36] N. Dhanachandra, K. Manglem, and Y. J. Chanu, "Image segmentation using K-means clustering algorithm and subtractive clustering algorithm," *Procedia Comput. Sci.*, vol. 54, pp. 764–771, Aug. 2015.
- [37] S. C. Satapathy, N. S. M. Raja, V. Rajinikanth, A. S. Ashour, and N. Dey, "Multi-level image thresholding using Otsu and chaotic bat algorithm," *Neural Comput. Appl.*, vol. 29, no. 12, pp. 1285–1307, 2016.
- [38] A. K. Bhandari, I. V. Kumar, and K. Srinivas, "Cuttlefish algorithm based multilevel 3D Otsu function for color image segmentation," *IEEE Trans. Instrum. Meas.*, to be published.
- [39] P. F. Felzenszwalb and D. P. Huttenlocher, "Efficient graph-based image segmentation," *Int. J. Comput. Vis.*, vol. 59, no. 2, pp. 167–181, Sep. 2004.
- [40] M. Zhang, H. Zhang, L. Wang, Y. Fang, J. Sun, and J. Li, "Supervised graph regularization based cross media retrieval with intra and inter-class correlation," *J. Vis. Commun. Image Represent.*, vol. 58, pp. 1–11, Jan. 2019.

- [41] D. Shi, L. Zhu, Z. Cheng, Z. Li, and H. Zhang, "Unsupervised multi-view feature extraction with dynamic graph learning," *J. Vis. Commun. Image Represent.*, vol. 56, pp. 256–264, Oct. 2018.
- [42] Y. Fang, H. Zhang, and Y. Ren, "Graph regularised sparse NMF factorisation for imagery de-noising," *IET Comput. Vis.*, vol. 12, no. 4, pp. 466–475, 2018.
- [43] X. Sui, Y. Zheng, B. Wei, H. Bi, J. Wu, X. Pan, Y. Yin, and S. Zhang, "Choroid segmentation from optical coherence tomography with graph-edge weights learned from deep convolutional neural networks," *Neurocomputing*, vol. 237, pp. 332–341, May 2017.
- [44] Y. Han, L. Zhu, Z. Cheng, J. Li, and X. Liu, "Discrete optimal graph clustering," *IEEE Trans. Cybern.*, to be published, doi: [10.1109/TCYB.2018.2881539](https://doi.org/10.1109/TCYB.2018.2881539).
- [45] J. Li, K. Lu, Z. Huang, L. Zhu, and H. T. Shen, "Heterogeneous domain adaptation through progressive alignment," *IEEE Trans. Neural Netw. Learn. Syst.*, vol. 30, no. 5, pp. 1381–1391, May 2019.
- [46] J. Li, K. Lu, Z. Huang, L. Zhu, and H. T. Shen, "Transfer independently together: A generalized framework for domain adaptation," *IEEE Trans. Cybern.*, vol. 49, no. 6, pp. 2144–2155, Jun. 2019.
- [47] X. Dong, H. Zhang, W. Wan, Z. Wang, Q. Wang, P. Guo, H. Ji, J. Sun, and L. Zhu, "Weighted locality collaborative representation based on sparse subspace," *J. Vis. Commun. Image Represent.*, vol. 58, pp. 187–194, Jan. 2019.
- [48] C. Cui, H. Liu, L. Nie, L. Zhu, Y. Yin, and T. Lian, "Distribution-oriented aesthetics assessment with semantic-aware hybrid network," *IEEE Trans. Multimedia*, vol. 21, no. 5, pp. 1209–1220, May 2019.
- [49] J. Sun, Y. Wang, J. Li, W. Wan, D. Cheng, and H. Zhang, "View-invariant gait recognition based on Kinect skeleton feature," *Multimed. Tools Appl.*, vol. 77, no. 19, pp. 24909–24935, 2018.
- [50] S. Hou, S. Zhou, Y. Zheng, and W. Liu, "Classifying advertising video by topicalizing high-level semantic concepts," *Multimedia Tools Appl.*, vol. 77, no. 19, pp. 25475–25511, 2018.
- [51] B. Zhang, L. Zhu, H. Zhang, and J. Sun, "Cross-media retrieval with collective deep semantic learning," *Multimedia Tools Appl.*, vol. 77, no. 17, pp. 22247–22266, 2018.
- [52] B. Liu, H. Liu, H. Zhang, and X. Qin, "A social force evacuation model driven by video data," *Simul. Model. Pract. Theory*, vol. 84, pp. 190–203, May 2018.
- [53] J. Zong, L. Meng, J. Zhang, Y. Ren, H. Zhang, and Y. Tan, "Adaptive reconstruction based multiple description coding with randomly offset quantizations," *Multimedia Tools Appl.*, vol. 77, no. 20, pp. 26293–26313, 2018.
- [54] J. Sun, X. Liu, J. Li, D. Zhao, H. Zhang, and W. Wan, "Video hashing based on appearance and attention features fusion via DBN," *Neurocomputing*, vol. 213, pp. 84–94, Nov. 2016.
- [55] B. Niu, D. Wang, N. D. Alotaibi, and F. E. Alsaadi, "Adaptive neural state-feedback tracking control of stochastic nonlinear switched systems: An average dwell-time method," *IEEE Trans. Neural Netw. Learn. Syst.*, vol. 30, no. 4, pp. 1076–1087, Apr. 2019.
- [56] B. Niu, Y. Liu, H. Li, P. Duan, J. Li, and W. Zhou, "Multiple Lyapunov functions for adaptive neural tracking control of switched nonlinear nonlower-triangular systems," *IEEE Trans. Cybern.*, to be published, doi: [10.1109/TCYB.2019.2906372](https://doi.org/10.1109/TCYB.2019.2906372).
- [57] Z. Wang, J. Xu, X. Song, and H. Zhang, "Consensus problem in multi-agent systems under delayed information," *Neurocomputing*, vol. 316, pp. 277–283, Nov. 2018.
- [58] L. Ma, X. Huo, X. Zhao, B. Niu, and G. Zong, "Adaptive neural control for switched nonlinear systems with unknown backlash-like hysteresis and output dead-zone," *Neurocomputing*, vol. 357, pp. 203–214, Sep. 2019.
- [59] C. Ji, C. Zhao, S. Liu, C. Yang, X. Meng, and L. Pan, "A just-in-time shapelet selection service for online time series classification," *Comput. Netw.*, vol. 157, pp. 89–98, Jul. 2019.
- [60] X. Dong, H. Zhang, W. Wan, and J. Sun, "A two-stage learning approach to face recognition," *J. Vis. Commun. Image Represent.*, vol. 43, pp. 21–29, Feb. 2017.
- [61] Y. Zhao, X. Zhao, Y. Liu, and Z. Xiang, "Online learning of dynamic multi-view gallery for person Re-identification," *Multimedia Tools Appl.*, vol. 76, no. 1, pp. 217–241, 2017.
- [62] Q. Mei, H. Zhang, and C. Liang, "A discriminative feature extraction approach for tumor classification using gene expression data," *Current Bioinf.*, vol. 11, no. 5, pp. 561–570, 2016.
- [63] F. Zhang and K. Zhang, "Superpixel guided structure sparsity for multi-spectral and hyperspectral image fusion over couple dictionary," *Multimedia Tools Appl.*, to be published, doi: [10.1007/s11042-019-7188-1](https://doi.org/10.1007/s11042-019-7188-1).
- [64] Y. Jiang, Y. Zheng, Y. Chang, J. Gee, and S. Hou, "Multimodal image alignment via linear mapping between feature modalities," *J. Healthcare Eng.*, vol. 2017, Jul. 2017, Art. no. 8625951.
- [65] L. Zhu, Z. Huang, Z. Li, L. Xie, and H. Shen, "Exploring auxiliary context: Discrete semantic transfer hashing for scalable image retrieval," *IEEE Trans. Neural Netw. Learn. Syst.*, vol. 29, no. 11, pp. 5264–5276, Nov. 2018.
- [66] L. Wang, L. Zhu, L. Liu, J. Sun, H. Zhang, and X. Dong, "Joint feature selection and graph regularization for modality-dependent cross-modal retrieval," *J. Vis. Commun. Image Represent.*, vol. 54, pp. 213–222, Jul. 2018.
- [67] J. Yan, H. Zhang, Q. Wang, P. Guo, L. Meng, W. Wan, X. Dong, and J. Sun, "Joint graph regularization based modality-dependent cross-media retrieval," *Multimedia Tools Appl.*, vol. 77, no. 3, pp. 3009–3027, 2018.
- [68] X. Dong, J. Sun, L. Meng, Y. Tan, W. Wan, H. Wu, B. Zhang, H. Zhang, and P. Duan, "Semi-supervised modality-dependent cross-media retrieval," *Multimedia Tools Appl.*, vol. 77, no. 3, pp. 3579–3595, 2018.
- [69] M. Zhao, H. Zhang, and L. Meng, "An angle structure descriptor for image retrieval," *China Commun.*, vol. 13, no. 8, pp. 222–230, 2016.
- [70] M. Zhao, H. Zhang, and J. Sun, "A novel image retrieval method based on multi-trend structure descriptor," *J. Vis. Commun. Image Represent.*, vol. 38, pp. 73–81, Jul. 2016.
- [71] I. K. Witus, C. K. On, A. Ibrahim, A. Ag, T. T. Guan, P. Anthony, and R. Alfred, "A review of computer vision methods for fruit recognition," *Adv. Sci. Lett.*, vol. 24, no. 2, pp. 1538–1542, 2018.
- [72] E. K. Nyarko, I. Vidović, K. Radočaj, and R. Cupec, "A nearest neighbor approach for fruit recognition in RGB-D images based on detection of convex surfaces," *Expert Syst. Appl.*, vol. 114, pp. 454–466, Dec. 2018.
- [73] J. Lu, W. Suk, H. Gan, and X. Hu, "Immature citrus fruit detection based on local binary pattern feature and hierarchical contour analysis," *Biosyst. Eng.*, vol. 171, pp. 78–90, Jul. 2018.
- [74] K. Hameed, D. Chai, and A. Rassau, "A comprehensive review of fruit and vegetable classification techniques," *Image Vis. Comput.*, vol. 80, pp. 24–44, Dec. 2018.
- [75] G. Lin, Y. Tang, J. Cheng, J. Xiong, and X. Zou, "Fruit detection in natural environment using partial shape matching and probabilistic Hough transform," *Precis. Agricult.*, to be published, doi: [10.1007/s11119-019-09662-w](https://doi.org/10.1007/s11119-019-09662-w).
- [76] A. Gungal, M. Karkee, and S. Amatya, "Apple fruit size estimation using a 3D machine vision system," *Inf. Process. Agricult.*, vol. 5, no. 4, pp. 498–503, 2018.



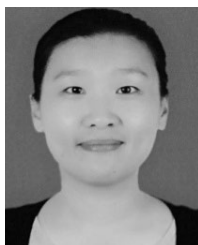
YUYU TIAN received the M.A. degree from Shandong Normal University. Her current research interests include artificial intelligence and agricultural information.



HUICHUAN DUAN received the Ph.D. degree. He is currently a Professor and a M.A. Supervisor with Shandong Normal University. His current research interests include artificial intelligence and robot control technology.



RONG LUO received the Ph.D. degree. She is currently an Associate Professor and a M.A. Supervisor with the Qilu University of Technology. Her current research interests include computational chemistry, biosensor, and smart material.



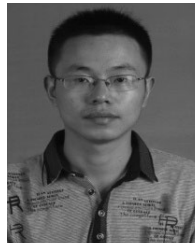
YAN ZHANG received the Ph.D. degree. She is currently a Lecturer with Shandong Management University. Her research interests include machine learning, machine vision, and image analysis.



YUANJIE ZHENG received the Ph.D. degree. He is currently a Professor and a Ph.D. Supervisor with Shandong Normal University. His research interests include artificial intelligence, machine learning, and smart medicine. He is a member of ACM, a Senior Member of CCF, and a CAAI member.



WEIKUAN JIA was born in 1982. He received the Ph.D. degree. He is currently an Associate Professor and a M.A. Supervisor with Shandong Normal University. His research interests include artificial intelligence, machine learning, and smart agriculture. He is a member of CCF and CAAI member.



CHENGZHI RUAN received the Ph.D. degree. He is currently an Associate Professor with Wuyi University. His research interests include image processing and robot control technology.



JIAN LIAN received the Ph.D. degree. He is currently a Lecturer with the Shandong University of Science and Technology. His current research interests include artificial intelligence, machine learning, and robot control technology.



CHENGJIANG LI received the Ph.D. degree. He is currently a Lecturer with the Shandong University of Science and Technology. His research interests include cluster analysis, machine learning, and robot control technology.

...